This paper first appeared in the sixteenth print edition of the *Photovoltaics International* journal, published in May 2012.

3D multi-physics modelling of unidirectional solidification of mc-Si in an ingot furnace

Anne J. Faber & **Adriaan M. Lankhorst**, CelSian Glass & Solar B.V., Eindhoven, The Netherlands, & **Bo Zhao** & **Cheng Wang**, Jinggong Science & Technology Co., Ltd, Zhejiang, China

ABSTRACT

Unidirectional solidification of large Si ingots from the melt phase is currently one of the most important technologies for producing mc-Si for PV cells. Si ingot furnaces began from casting equipment, and have been improved by DSS (directional solidification system) or DSS-like methods. To improve PV cell efficiency and reduce costs, intensive development has focused on increasing a single ingot's volume, reducing impurities and controlling the growth speed and temperature gradient. One of the latest developments of Si ingot furnaces is mono-like crystalline silicon growth using a seed preservation method and more accurate control. The Si ingot furnaces are optimized with precise control of temperature gradients and growth speed for the formation of a large unit of quasi-monocrystalline Si. This optimization can further improve a PV cell's efficiency by at least 1%. In order to obtain fundamental knowledge about the key process steps that determine the growth and electrical quality of mc-Si via directional solidification in an ingot furnace, a combined modelling-measuring approach is essential. Moreover, a mathematical model of the Si ingot casting process can be used for model-based process control.

Introduction

In the first part of this paper, the underlying physical phenomena and physical laws of the Si ingot process are explained on the basis of characteristic dimensionless numbers. The equations for the physical laws are solved numerically in X-stream – CelSian's dedicated 3D computational fluid dynamics (CFD) package. X-stream is a multi-physics CFD package with sub-models representing, for example, flow, melting, radiation heat transfer, turbulence, combustion, kinetic reactions and thin-layer deposition [1,2]. The solver in X-stream is based on the finite volume method as described in Ferziger & Peric [3], the grids are 3D multi-block structured and body fitted, and the code is fully parallelized. Typical results of 3D CFD modelling calculations are presented in the second part of this paper.

Figure 1. Cross section of Jinggong's mono-like crystalline ingot (height 100mm).

Figure 2. Jinggong assembly line for the JJL500N Si ingot furnace.

Physical characteristics of the Si solidification process

Fig. 3 shows a simplified configuration of a Si ingot furnace: a rectangular quartz crucible, containing the Si load, is placed in a rectangular housing of insulating refractory material. Usually, the bottom of this housing is formed by a water-cooled copper plate. The area around the crucible is flushed with argon gas. The batch process begins with the filling of the crucible with Si chunks and heating them well above the melting temperature of Si to form a Si melt. The unidirectional crystallization process is started by increasing the heat loss via the crucible bottom, with the help of the water-cooled bottom plate, and lowering the power of the heaters, causing a vertical temperature gradient in the Si melt. In this way, solidification starts at the bottom and proceeds upwards until no melt is left.

The physical phenomena that play a role in these industrial Si ingot furnaces include:

- Heat transfer by conduction, convection and radiation from the heaters to the Si load, within the Si load and from the Si load to the cooled crucible bottom.
- Flows and transport of chemical species in the Si melt as well as in the argon gas above the melt.

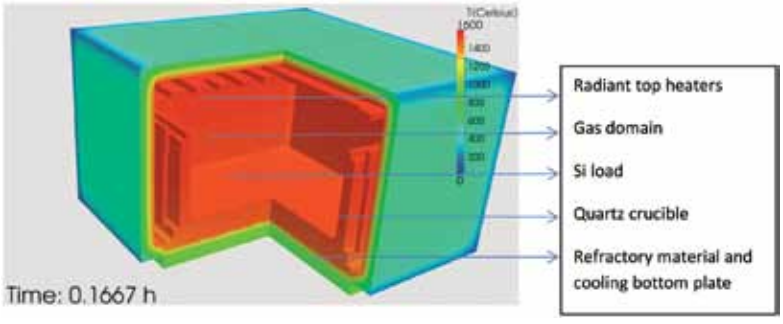

Figure 3. Simplified schematic of a Si ingot furnace, showing different physical domains.

- Release of latent heat by the Si during crystallization.

> "Natural convection and turbulent flow must be taken into account for the flow patterns in the very low viscosity Si melt to be correctly described."

The most important physical features of the Si ingot process can be identified by considering some key dimensionless numbers that characterize the heat transfer, the mass flow, and the liquid–solid phase change in the system. Table 1 summarizes the most relevant physical characteristics of Si for this process, as well as the characteristics of water for comparison. By estimating the values of the physical numbers, as given in this table, the following general conclusions for the directional Si crystallization process can be derived:

- Since the Stefan number (the ratio between sensible heat and latent heat) is small, the Si solidification process is dominated by the latent heat release given by

$$k_{Si_m}\frac{dT}{dy}\Big|_m - k_{Si_c}\frac{dT}{dy}\Big|_c = \rho H R_{Si} \quad (1)$$

where H is latent heat, ρ is silicon density, and k_{Si_m} and k_{Si_c} are the melt and crystal thermal conductivities respectively. The Si solidification process is characterized by the crystallization rate $R_{Si} = \frac{dy}{dT}$.

- From the formula in Equation 1, the order of magnitude of the Si solidification rate in the stationary situation can be estimated to be $R_{Si} \approx 1.0$cm/hr.

- At the onset of crystallization (at the bottom of the ingot), the temperature in the top layers of the Si melt is assumed to be about 1460°C.

- Natural convection and turbulent flow must be taken into account for the flow patterns in the very low viscosity Si melt to be correctly described.

- Although typical Si flow velocities are small (of the order of mm/s – see Table 1), the heat transfer in the liquid Si is dominated by convective heat transfer, as the thermal Péclet number is much larger than unity.

Besides these guidelines for the Si domain, the following physical phenomena in the gas domain should be accounted for: laminar or turbulent flow in the gas, and heat transport from the heaters to the Si load by (mainly) radiation. Taking these into consideration, in order to simulate numerically the complete Si solidification process in an ingot furnace by

Properties @ T_m	Symbol	Unit	Silicon	Water	Remarks
Melting temperature	T_m	°C	1414.00	0	
Melting temperature	T_m	K	1687.15	273.15	
Heat capacity	C_p	J/kgK	910.0	4221.0	Water has by far the highest heat capacity
Thermal conductivity	k	W/mK	56.5	0.55	Silicon is much more conductive than water
Density	ρ	kg/m^3	2583	1000	
Dynamic viscosity	η	kg/ms	5.57E-04	1.79E-03	Liquid silicon is less viscous than water
Kinematic viscosity	ν	m^2/s	2.16E-07	1.79E-06	
Thermal expansion coefficient	β	1/K	7.17E-05	7.00E-05	Of the same order for silicon and water
Latent heat	H	J/kg	1.79E+06	2.50E+06	High latent heat for both silicon and water
Gravity	g	m/s^2	9.81	9.81	
Characteristic temperature difference	ΔT	K	10	10	
Characteristic dimension	L	m	0.25	0.25	
Stefan number	Ste	-	5.08E-03	1.69E-02	The smaller the Stefan number, the more that latent heat effects dominate; Si solidification largely dominated by H
Prandtl number	Pr	-	8.97E-03	1.37E+01	Molten Si: hydrodynamic boundary layer much smaller than thermal boundary layer
Grashof number	Gr	-	2.36E+09	3.34E+07	The higher the Grashof number, the stronger the natural convection
Rayleigh number	Ra	-	2.12E+07	4.58E+08	Turbulent flow for Ra > 10^6–10^9
Péclet number	Pe	-	109	5370	Ratio of heat transfer by convection versus conduction
Buoyant velocity scale	V_b	m/s	4.19E-02	4.14E-02	
Maximum velocity in boundary layer	V_{max}	m/s	1.05E-02	2.80E-03	Pr < 1: $V_{max} \approx 0.25 * V_b$ Pr > 1: $V_{max} \approx 0.25 * Pr^{-0.5} * V_b$
Dimensionless distance from velocity maximum to wall	x/L	-	2.21E-03	1.03E-03	
Distance from velocity maximum to wall	x	m	5.53E-04	2.56E-04	Very thin (of the order 0.5mm) boundary layers in both cases

Table 1. Physical properties and characteristic numbers of Si compared to water.

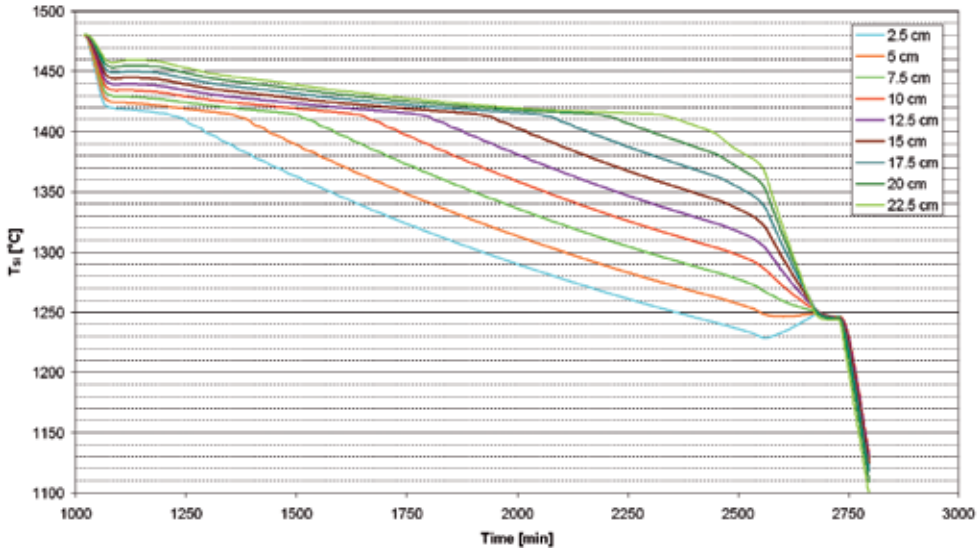

Figure 4. Calculated Si melting temperatures at various vertical positions (distance from the crucible bottom).

a CFD model, the simulation model should involve:

- solving the equations governing the energy conservation laws in all domains (gas, Si and refractory materials);
- solving the laminar or turbulent flow equations in the gas domain surrounding the ingot;
- determining the natural convection and turbulent flows in the Si melt domain;
- solving for detailed radiative heat transfer (discrete ordinates model) in the gas domain surrounding the ingot.

Typical 3D-modelling results for an industrial Si ingot furnace are presented next.

3D simulations of an mc-Si ingot furnace

Full-scale calculations were conducted for one quarter of an industrial 410kg-ingot mc-Si ingot furnace. The grid for this geometry consists of 0.5 million hexahedral grid cells, of which roughly 20% are located in the silicon melt (typical melt cell size 10mm × 6mm × 10mm). The geometry is subdivided into several domains, each domain having a different set of sub-models applied for different physics. Here, the domains are silicon, quartz and support crucibles, refractory housing and the argon-filled space between the box and the housing; each heater is also a separate domain. The energy equation is solved in all domains: the enthalpy formulation is used on the silicon domain, and the usual temperature formulation on the other domains. The solutions are coupled over domain boundaries to ensure continuity of temperature and heat fluxes. Radiative heat transfer in the gas domain is solved by a discrete ordinates model. Laminar flow equations are solved in the argon-gas space.

During crystallization, the heater power and the water cooling are controlled in such a way that the temperature signals from three thermocouples follow a target curve in time. During a specific test run, to locate the crystallization front as a function of time, dip-rod measurements were taken at two positions in the melt: one in the centre, and the other in the corner of the crucible.

Transient heater power and bottom water cooling-rate data were used as input for the model. The model was validated by comparing the transient results with the temperatures of the three thermocouples as well as of the front positions at the two dip-rod locations.

> "As a result of the huge amount of latent heat release, temperatures close to the actual crystallization front remain close to the Si melting temperature (1414°C)."

Simulations were carried out with and without Si melt flow enabled. Fig. 4 shows the calculated temperatures for the case of no Si melt flow, at nine vertically distributed centre points in the Si melt. As a result of the huge amount of latent heat release, temperatures close to the actual crystallization front remain close to the Si melting temperature (1414°C). For points located in the solid crystal, the temperature rapidly decreases because of the heat removal by the bottom cooling plate. Compared to temperature gradients in the crystal, gradients in the melt are small owing to the higher thermal conductivity of liquid Si (k_{Si_m} = 56.5W/mK) compared to the solid Si thermal conductivity, which is given by:

$$k_{Si_c}(T)=1.21\cdot10^{5}\cdot T^{-1.1921} \quad (2)$$

where T is the temperature in K. At the melting temperature, k_{Si_c} = 17.2W/mK [4].

In Fig. 5 the front positions calculated without melt flow enabled are compared to the dip-rod measurements. As regards the front positions, the agreement on the centre line of the ingot is excellent, whereas the predictions in the corner are somewhat less accurate. The calculations predict a planar (slightly concave) front (as seen from the crystal), but the dip-rod measurements indicate that in reality the surface is convex. Comparison of the front shapes between melt-flow and no-melt-flow calculations after five hours' process time suggests that the convexity is reproduced better when melt flow is switched on in the model.

The small temperature gradients involved make this process very sensitive to process parameters, but, bearing that in mind, the qualitative agreement between measurements and calculations is quite good. Once crystallization starts and latent heat is released at the front, the removal of this latent heat is much more important for the energy flows in the silicon than the removal of the sensible heat, as shown earlier in Table 1 by the low value of the silicon Stefan number.

Fig. 6 shows a snapshot of the (transient) flow pattern on the boundary of the Si melt for the first five hours of the process in the case when a laminar flow model is used. The flow field is the superposition of a large loop and smaller convection cells that vary in size and position during crystallization. The flow is driven by the

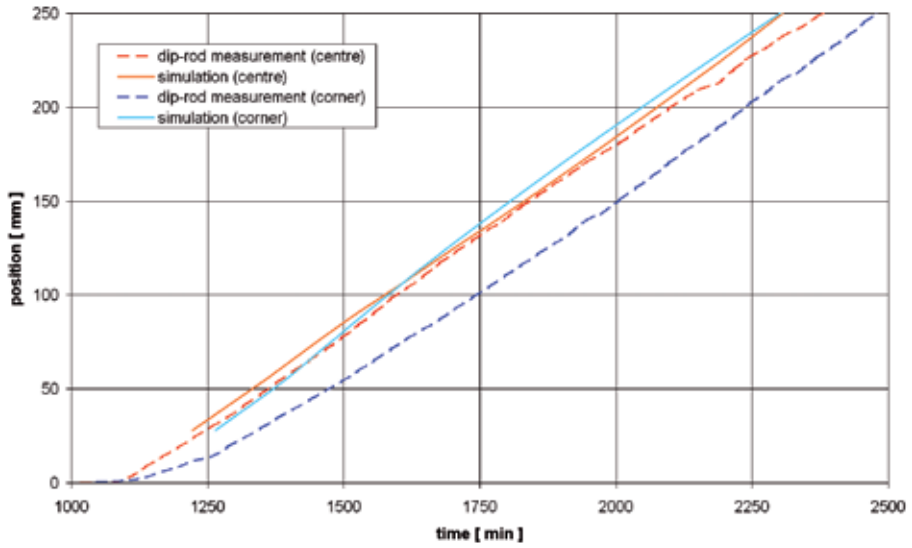

Figure 5. Measured and calculated positions of the Si crystallization front at two locations (centre and corner).

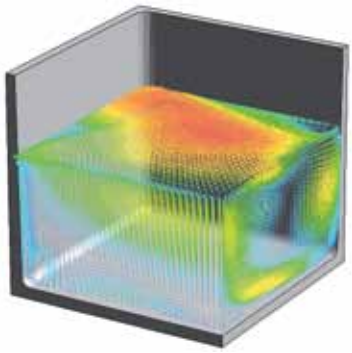

Figure 6. Snapshot of velocity vectors on the boundary of the silicon domain.

deviations from the stratified temperature/density profile, due to the release of latent heat at the front, the developing front curvature and the non-adiabatic side walls.

"The model is ready to support ingot furnace design and can ultimately be used in model-based crystallization process control."

Conclusions

Several basic physical processes interact in a subtle manner in industrial ingot furnaces for the crystallization of mc-Si via the vertical temperature-gradient method. The required components are: flow of melt and gas; energy transport through conduction, convection and radiation; and release of latent heat and solidification. These aspects have been implemented in X-stream – CelSian's dedicated 3D multi-physics multi-domain CFD simulation package.

The results for a complete, industrial 3D mc-Si furnace have been presented. For this furnace, where actual transient heater-power curves provided the main input for the model, the calculated thermocouple temperatures at locations just outside the silicon showed maximal differences of 10–20°C from the measurements. From this it may be concluded that the general energy flows in the complete furnace were well captured by the model. This means that the model can be used to gain insight into the process to investigate the effects of various interacting physical phenomena – radiation, convection, latent heat release, flow, etc. Furthermore, the model is ready to support ingot furnace design and can ultimately be used in model-based crystallization process control.

References

[1] Thielen, L. et al. 2007. "Simulation of multiphysical phenomena in glass melting furnaces", *Proc. NAFEMS World Congr.*, Vancouver, Canada.

[2] Lankhorst, A.M. et al. 2007. "Transient ALD simulations for a multi-wafer reactor with trenched wafers", *Surf. Coat. Techn.*, Vol. 201, pp. 8842–8848.

[3] Ferziger, P. & Peric, M. 2002. *Computational Methods for Fluid Dynamics*, 3rd ed. Berlin Heidelberg: Springer.

[4] Yamasue, E. et al. 2002. "Thermal conductivities of silicon and germanium in solid and liquid states measured by non-stationary hot wire method with silica coated probe", *J. Cryst. Growth*, Vol. 234, pp. 121–131.

About the Authors

Anne Jans Faber completed his studies in experimental physics at Utrecht State University, The Netherlands, in 1985, and is a senior scientist at CelSian Glass & Solar (formerly TNO Glass Group) in Eindhoven. He works as a contract researcher for international companies in the fields of glass science and technology, high-temperature sensors and solar silicon processes. Anne has authored/co-authored numerous scientific publications, and is the holder of several patents.

Adriaan Lankhorst received his doctoral degree in applied physics from Delft University of Technology, The Netherlands, in 1991, and is an R&D manager at CelSian Glass & Solar. He started working at TNO in 1990 as a process physicist, managing and executing projects involving complex physics and chemistry and the development and application of CFD models. Adriaan specializes in high-temperature processes such as glass melting, as well as combustion, turbulence, radiation, and mc-Si processes.

Bo Zhao is the CTO of Jinggong Science & Technology Co. Ltd. and the GM of Jinggong Mechatronic Research Institute. Bo has specialized in automatic control and crystal growth of silicon ingot furnaces for more than 10 years, and has led a number of key innovations in hot-zone design and crystal growth processes.

Cheng Wang is an R&D manager at Jinggong Mechatronic Research Institute. A CAE engineer specializing in numerical simulation for silicon ingot furnace design, Cheng is currently focusing on theoretical research into silicon crystal growth.

Enquiries

Anne Jans Faber
Tel: + 31 6 22973991
Email: anne-jans.faber@celsian.nl